RAPID COMMUNICATIONS

PHYSICAL REVIEW B **92**, 220408(R) (2015)

Electronic phase transition in hollandite titanates $Ba_xTi_8O_{16+\delta}$

R. Murata,[1] T. Sato,[1] T. Okuda,[2] Y. Horibe,[3] H. Tsukasaki,[4] S. Mori,[4] N. Yamaguchi,[1] K. Sugimoto,[5]
S. Kawaguchi,[5] M. Takata,[5] and T. Katsufuji[1,6,*]

[1]*Department of Physics, Waseda University, Tokyo 169-8555, Japan*
[2]*Department of Nano-structures and Advanced Materials, Kagoshima University, Kagoshima 890-0065, Japan*
[3]*Department of Materials Science and Engineering, Kyushu Institute of Technology, Kitakyushu 804-8550, Japan*
[4]*Department of Materials Science, Osaka Prefecture University, Sakai 599-8531, Japan*
[5]*Japan Synchrotron Radiation Research Institute, Hyogo 679-5198, Japan*
[6]*Kagami Memorial Research Institute for Materials Science and Technology, Waseda University, Tokyo 169-0051, Japan*

(Received 12 August 2015; revised manuscript received 9 November 2015; published 14 December 2015)

We studied the physical properties of hollandite titanates, $Ba_xTi_8O_{16+\delta}$, which have double chains of edge-sharing TiO_6 octahedra with d electrons in the t_{2g} states. We found that there is an electronic phase transition at $\sim$220 K, at which various properties exhibit anomalies. This phase transition is characterized by a modulation in the TiO_6 chains and a spectral weight transfer of over 2 eV in the optical conductivity spectrum, which are presumably caused by charge and orbital ordering of the Ti t_{2g} electrons.

DOI: 10.1103/PhysRevB.92.220408 PACS number(s): 75.25.Dk, 61.05.J−, 72.20.Pa, 78.30.−j

It is known that quasi-one-dimensional (1D) conductors often exhibit a characteristic ground state, charge density wave (CDW) [1], arising from the nesting of the Fermi surface. It is an interesting issue how this ordered state is modified if the effect of electron correlation is added. In reality, however, there are not many 1D conductors in 3d transition-metal oxides having strong electron correlation, since many of them with 1D structures become good insulators. There are several examples in copper oxides based on the d^9 electron configuration. $Sr_{14-x}Ca_xCu_{24}O_{41}$ [2,3] has Cu ladders and becomes conducting with hole doping into the Cu ions by increasing x. The ordering of the Cu holes was observed by resonant x-ray scattering [4], though it barely affects the macroscopic properties. $PrBa_2Cu_4O_8$ [5,6] has a conducting Cu double chains and is metallic down to the lowest T. There are also several examples of the 1D conductors with transition metals on the left side of the periodic table, thus having a small number of d electrons. For example, β-$Na_{0.33}V_2O_5$ [7,8] with 0.17 d electrons per V exhibit a phase transition at $T_c = 136$ K with a tripling of the unit cell along the 1D direction. The resistivity sharply increases but the magnetic susceptibility exhibits only a small anomaly at T_c. The optical measurement indicates a gap opening and an evolution of a peak at $\sim$0.4 eV below T_c [9], which is similar to the behavior of conventional CDW compounds [1].

Recently, it has been reported that transition-metal oxides with a hollandite structure exhibits intriguing phase transitions [10–16]. The hollandite structure $A_2B_8O_{16}$ is characterized by double chains consisting of edge-sharing BO_6 octahedra (as illustrated in the upper panel of Fig. 1). For $K_2V_8O_{16}$, in which the average valence of the V ions is +3.75 (1.25 d electrons per V), a structural phase transition occurs at 170 K, where the resistivity jumps by two orders of magnitude and the magnetic susceptibility is suppressed [10]. It was experimentally shown that charge segregation and V dimerization with a spin-singlet state in the chains are the origin of the phase transition at 170 K [11]. $K_2Cr_2O_{16}$, in which there are 2.25 d electrons per Cr, exhibits a ferromagnetic ordering at 180 K and a metal-insulator transition at 95 K [12]. Theoretically, it has been proposed that this metal-insulator transition in the ferromagnetic phase is caused by a Peierls instability in the fully spin-polarized state [14].

The number of d electrons per transition metal in holladiate vanadate and chromate described above is larger than unity, and for comparison, it is important to study the physical properties of hollandite compounds with diluted d electrons. For this purpose, hollandite titanates [17–19], in which the number of d electrons per Ti is less than unity, are good candidates, though their physical properties have not yet been well studied. In the present study, we investigated single crystals of $Ba_xTi_8O_{16+\delta}$ and found an exotic phase transition at $\sim$220 K.

Single crystals of $Ba_xTi_8O_{16+\delta}$ were grown by the floating-zone technique. $BaTiO_3$, TiO_2, and Ti were mixed and pressed into a rod, which was directly melted in a floating-zone furnace in a flow of two different gases, Ar and H_2-7%/Ar. We found that the crystals grown in Ar gas are tetragonal whereas those grown in H_2-7%/Ar gas are monoclinic at room temperature. We also estimated the ratio of Ba, Ti, and O by induction-coupled plasma analysis and thermogravimetric analysis and found that, for the notation $Ba_xTi_8O_{16+\delta}$, $x = 1.06$ and $\delta = 0.35$, and thus the nominal number of electrons per Ti (n) is 0.18 for the No. 1 tetragonal sample; $x = 1.13$, $\delta = 0.14$, and $n = 0.25$ for the No. 2 tetragonal sample; and $x = 1.13$, $\delta = -0.49$, and $n = 0.40$ for the monoclinic sample [20]. Since we observed a phase transition only in the tetragonal samples, we mainly discuss their results below and discuss the result of the monoclinic sample in the Supplementary Material [21].

The resistivity was measured by a four-probe technique. The magnetization was measured using a SQUID magnetometer. The thermopower and thermal conductivity were simultaneously measured by a steady-state method. The optical reflectivity was measured between 0.01 and 0.8 eV using an FTIR spectrometer and between 0.7 and 5 eV using a grating spectrometer on polished surfaces. The Raman scattering was measured by a technique described elsewhere [22]. A synchrotron x-ray powder diffraction measurement was

---

[*] To whom correspondence should be addressed.

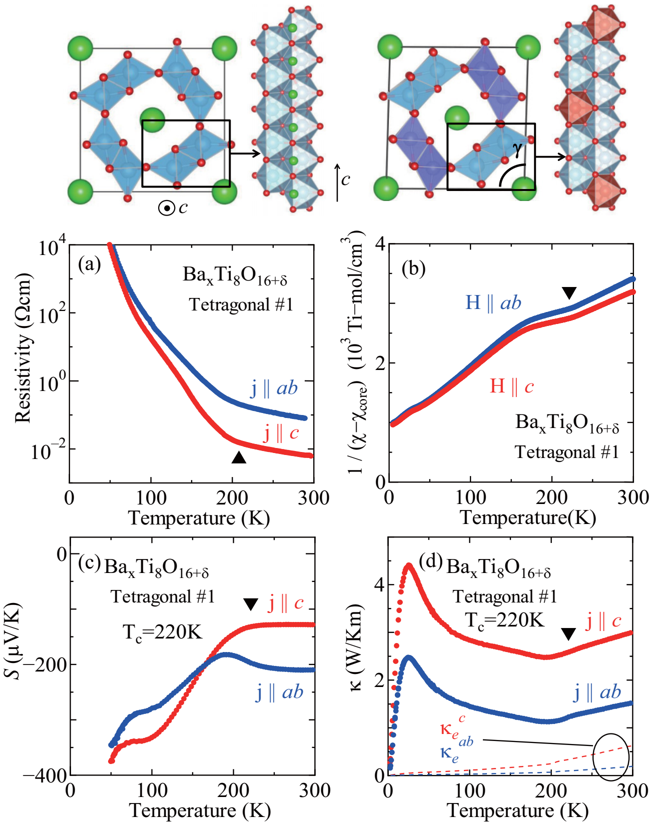

FIG. 1. (Color online) (Top) Crystal structures of the tetragonal (left) and monoclinic (right) phase. The crystal structure was drawn by VESTA [24]. (a) and (b) Temperature dependence of (a) resistivity, (b) inverse magnetic susceptibility, (c) Seebeck coefficient, and (d) thermal conductivity for tetragonal $Ba_xTi_8O_{16+\delta}$ (No. 1) along the *c* axis (parallel to the double chains) and the *ab* axis (perpendicular to the chains).

performed with an incident wavelength of 0.7745 Å at SPring-8 BL02B2 [23]. Electron diffraction experiments were carried out in a temperature window between 298 and 115 K in a JEM-2010 transmission electron microscope.

Figure 1(a) shows the temperature (T) dependence of the resistivity ρ for $Ba_xTi_8O_{16+\delta}$ with a tetragonal structure at room temperature (No. 1). The resistivity along the c axis (parallel to the chains), ρ_c, is 1–2 orders of magnitude smaller than that along the a axis (perpendicular to the chains), ρ_a, indicating a modest one-dimensional character of the electrical conduction. Both ρ_c and ρ_a exhibit an anomaly at ~220 K, below which ρ_c increases with decreasing T from 10^{-2} Ωcm to more than 10^4 Ωcm. This suggests the existence of a phase transition at 220 K and the opening of a charge gap below the transition temperature.

The inverse magnetic susceptibility $1/(\chi - \chi_{\rm core})$ of $Ba_xTi_8O_{16+\delta}$ (No. 1) as a function of T is shown in Fig. 1(b). ($\chi_{\rm core}$ is the T-independent diamagnetic susceptibility of this compound, -4.8×10^{-5} cm^3/Ti mol.) This T dependence also indicates the existence of an anomaly at ~220 K. The magnetic susceptibility obeys the Curie-Weiss law, $\chi - \chi_{\rm core} = C/(T+\theta)$, both above 220 K ($C = 0.171$ K cm^3/Ti mol and $\theta = 244$ K) and below 150 K ($C = 0.092$ K cm^3/Ti mol and $\theta = 71$ K) with different Curie constants C and Weiss temperatures θ [25]. Note that the absolute values of C below 150 K are comparable to the value of 0.068 K cm^3/Ti mol expected if $n = 0.18$ d electrons per Ti are localized and act as $S = 1/2$ spins. The Weiss temperature below 150 K indicates a modest size of an antiferromagnetic interaction between the localized magnetic moments.

Figures 1(c) and 1(d) show the T dependence of the Seebeck coefficient (S) and the thermal conductivity (κ) for $Ba_xTi_8O_{16+\delta}$ (No. 1). The sign of S is negative and almost independent of T above ~220 K with relatively large absolute values (~ − 120 and ~ − 200 μV/K along the c and a axes, respectively). These results are consistent with the fact that this compound is conducting above ~220 K but the nominal number of d electrons per Ti is relatively small (n~0.18). As to the anisotropy of S ($|S_a| > |S_c|$), unlike the case of the electrical conductivity, the anisotropy of S is not directly correlated to the anisotropy of the effective mass theoretically. Experimentally, the absolute value of S often becomes larger in the direction along which the resistivity is higher [26,27], similarly to the present compound. It also should be pointed out that the so-called generalized Heikes formula [28], considering the threefold degeneracy of the t_{2g} orbitals, gives $S = -(k_B/e)\ln[6(1-n)/n] \sim -285$ μV/K, which is comparable to S_a experimentally obtained. Below ~220 K, the absolute value of the Seebeck coefficient increases with decreasing T and amounts to ~ − 400 μV /K. This indicates that the number of carriers decreases below 220 K.

The anomaly at 220 K also exists in the T dependence of the thermal conductivity, as shown in Fig. 1(d). Above 220 K, the thermal conductivity decreases with decreasing T, and below 220 K, the thermal conductivity first exhibits a small additional decrease but then increases with further decreasing T below 200 K. In the same figure, the electron thermal conductivity (κ_e) obtained from the electrical conductivity (σ) [the inverse of ρ shown in Fig. 1(a)] with the Wiedemann-Franz relation $\kappa_e = (\pi^2/3)(k_B/e)^2 T\sigma$ is shown by dashed lines. As can be seen, the anomaly observed around 220 K in the thermal conductivity cannot be explained by the electron thermal conductivity and thus, it should be attributed to the change in the phonon thermal conductivity with T.

To investigate the anomaly at 220 K from the viewpoint of the crystal structure, we measured the synchrotron powder x-ray diffraction. It was found that some of the diffraction peaks are split below 220 K [Fig. 2(a)], which can be interpreted as a structural phase transition from tetragonal to monoclinic with the same symmetry as the monoclinic sample, as shown in Fig. 2(b). We also measured the Raman scattering of tetragonal $Ba_xTi_8O_{16+\delta}$ with the incident light of $\hbar\omega = 2.41$ eV, and the spectra with the polarization directions along the c axis for both incident and scattered light [the (cc) polarization configuration] are shown in Fig. 2(c). As can be seen, many peaks evolve below T_c whose intensities are much larger than those in the (aa) polarization spectrum shown in the same figure. According to group theory analysis, 6 and 12 A_g modes exist in the tetragonal and monoclinic phases, respectively, but in all of them the atoms move along the ab plane but not along the c axis. It is unlikely that all of such modes are observed only in the cc polarization spectrum but

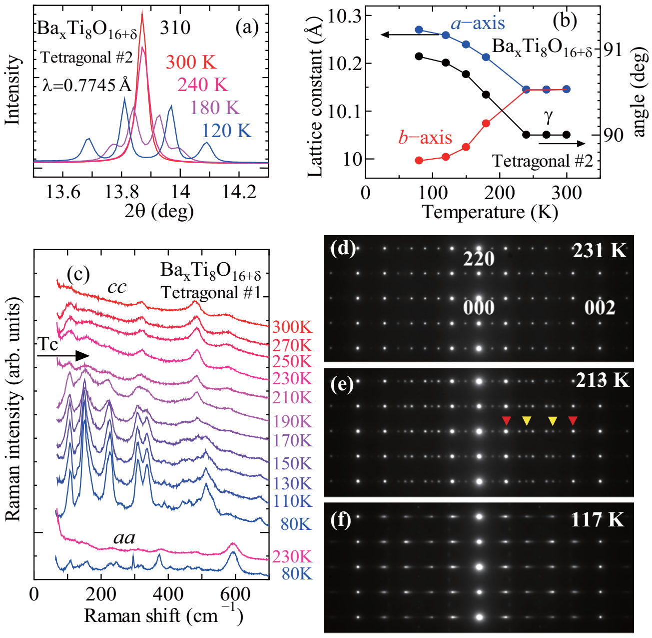

FIG. 2. (Color online) (a) Synchrotron x-ray powder diffraction pattern around the (310) peak for No. 2 tetragonal $Ba_xTi_8O_{16+\delta}$, and (b) T dependence of lattice parameters (a, b, and the monoclinic angle γ) obtained from x-ray diffraction. (c) Raman scattering spectra for No. 1 tetragonal $Ba_xTi_8O_{16+\delta}$ with the polarization directions along the c axis for both the incident and scattered light, (cc), and those along the a axis, aa. (d), (e), and (f) Electron diffraction patterns of No. 1 tetragonal $Ba_xTi_8O_{16+\delta}$ taken from the $[1\bar{1}0]$ direction.

not observed at all in the aa polarization spectrum, unless strong resonance effect exists, which is also unlikely.

To obtain information about such a small structural change, we performed electron diffraction measurement on $Ba_xTi_8O_{16+\delta}$. Figures 2(d), 2(e), and 2(f) show the electron diffraction patterns at various temperatures taken from the $[1\bar{1}0]$ direction. As can be seen, superlattice peaks exist along the $(00l)$ direction even above T_c, which divide the span between the (000) and (002) peaks into nine, i.e., the peaks are located at $(00\frac{2n}{9})$ [Fig. 2(d)]. Below T_c, additional superlattice peaks appear at the midpoint between the neighboring peaks, i.e., at $(00\frac{n}{9})$ [Fig. 2(e)]. Note that among the $(00\frac{n}{9})$ peaks, $n =$ 7 and 11 (shown by yellow triangles) have larger intensities. With further decreasing T, the $(00\frac{n}{9})$ peaks with $n = 7$ and 11 and the $(00\frac{2n}{9})$ peaks with $n = 2$ and 7 [shown by red triangles in Fig. 2(e)], i.e., the $(00l)$ peaks with $l = 4/9$, 7/9, 11/9, and 14/9 maintain their intensities but change into diffuse peaks [Fig. 2(f)]. Note that these l values are close to $2n/5$ with $n = 1$–4 [29].

Superlattice structures along the chain direction are often observed in hollandite compounds, which arise from the ordering of the A-site ions [30]. For $Ba_xTi_8O_{16+\delta}$, $x = 2$ corresponds to the stoichiometric composition and thus, only a half the sites are occupied by Ba ions in the No. 1 tetragonal crystals ($x = 1.06$). Thus the ordering of the Ba ions is possible, resulting in the superlattice peaks above T_c at $(00\frac{2n}{9})$. On the other hand, the $(00\frac{n}{9})$ peaks appearing below T_c can be attributed to an electronic phase transition occurring at $T_c = 220$ K, which induces a modulation in the electronic structure of the Ti d states. The fact that only the $(00l)$ peaks with $l = 4/9$, 7/9, 11/9, and 14/9 survive as diffuse peaks at lower T suggests that the superlattice peaks arising from the modulation of the d electrons in the Ti chain should be at $(00\frac{2n}{5})$, but the locking of the modulation occurs in the presence of ninefold modulation for the Ba ions, whereas the ordering of the Ba ions itself is modulated by the modulation in the Ti chain.

There are several differences between the present compounds and conventional CDW compounds. In the latter case, the magnetic susceptibility decreases at the transition temperature, but at lower T, it exhibits T-independent behavior arising from Pauli paramagnetism and Larmor diamagnetism [31]. However, the magnetic susceptibility of $Ba_xTi_8O_{16+\delta}$ exhibits a Curie-Weiss behavior even below the transition temperature $T_c = 220$ K, as shown in Fig. 1(b). Furthermore, the decrease in the thermal conductivity with decreasing T above T_c and its increase with decreasing T below T_c [Fig. 1(d)] is not a typical behavior of CDW compounds [32–34]. Instead, it is observed in strongly correlated electron systems exhibiting orbital ordering [35–37]. In such systems, acoustic phonons, by which heat is carried, are scattered by an orbital fluctuation above the transition temperature, resulting in a decrease in thermal conduction, whereas a long-range orbital ordering suppresses the orbital fluctuation below the transition temperature, resulting in an increase in thermal conduction.

To understand this phase transition at 220 K from the viewpoint of the electronic structure, the optical reflectivity spectra of tetragonal $Ba_xTi_8O_{16+\delta}$ (No. 2) were measured and converted to optical conductivity spectra $\sigma(\omega)$ by the Kramers-Kronig transformation. Figure 3(a) shows the optical reflectivity spectra with the polarization along the c axis and

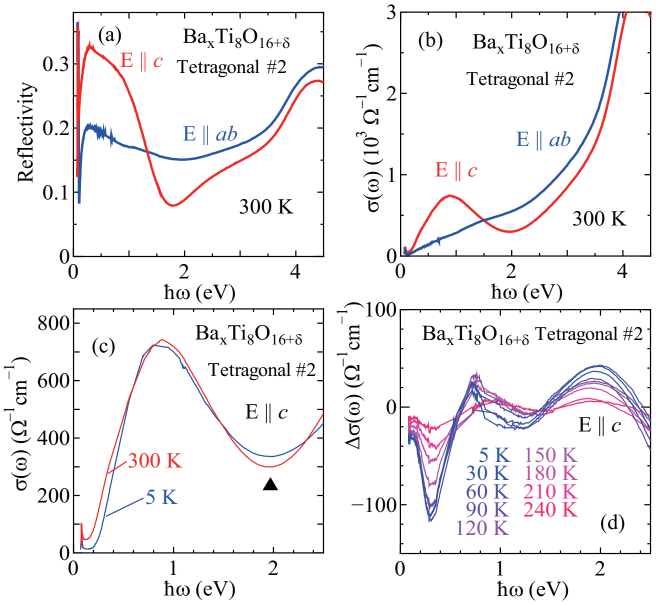

FIG. 3. (Color online) (a) Reflectivity and (c) optical conductivity spectra for tetragonal $Ba_xTi_8O_{16+\delta}$ (No. 2) at room temperature with the polarization direction along the c axis and ab plane. (c) Optical conductivity spectra and (d) optical conductivity difference spectra $[\sigma_T(\omega) - \sigma_{300K}(\omega)]$ for No. 2 tetragonal $Ba_xTi_8O_{16+\delta}$ along the c axis at various temperatures.

along the *ab* plane. An edge at ~1.8 eV and an increase below this energy are observed only in the *c*-axis reflectivity spectrum. In the optical conductivity spectra [Fig. 3(b)], a peak structure centered at ~1 eV exists in $\sigma_c(\omega)$, whereas such a structure is absent in $\sigma_a(\omega)$. On the basis of the crystal structure of the present compound, it is reasonable to assign this peak at ~1 eV to the conducting *d* electrons of the Ti ions along the double chains. The contribution of such conducting *d* electrons along the chain does not produce a Drude spectrum but produces a peak structure, probably because the conducting carriers are trapped by lattice distortion and form small polarons even above T_c. The peak at 4 eV existing both in $\sigma_c(\omega)$ and $\sigma_a(\omega)$ is attributed to charge-transfer excitation from the oxygen $2p$ level to the Ti $3d$ level.

Figure 3(c) shows the $\sigma_c(\omega)$ spectra at 300 and 5 K. With decreasing T, σ_c below 1 eV decreases, whereas the valley in the $\sigma_c(\omega)$ spectrum at ~2 eV is filled. Note that this is different from the conventional behavior of optical spectra, in which peaks narrow and the valley should deepen with decreasing T. Figure 3(d) shows the $\sigma_c(\omega)$ difference spectrum, $\sigma_c(\omega)_T - \sigma_c(\omega)_{300\mathrm{K}}$. As can be seen, dips at ~0.4 and ~1 eV develop whereas a peak develops at ~2 eV with decreasing T. We point out that in conventional CDW compounds, the energy scale of the spectral weight transfer in the optical conductivity spectrum is usually much lower than 1 eV [38,39], and this is the case for β-$\mathrm{Na}_{0.33}\mathrm{V}_2\mathrm{O}_5$. The anomalously large energy scale (~2 eV) in the spectral weight transfer associated with the phase transition in $\mathrm{Ba}_x\mathrm{Ti}_8\mathrm{O}_{16+\delta}$ indicates an important role of the electron correlation effect for this phase transition, similarly to the charge/orbital ordering in magnanites [40].

These experimental results indicate that the phase transition at 220 K in $\mathrm{Ba}_x\mathrm{Ti}_8\mathrm{O}_{16+\delta}$ is caused by the charge and orbital ordering of the Ti $3d$ electrons, which induces a modulation of the crystal structure along the Ti chain. A possible charge ordering pattern consistent with the approximate five-fold modulation along the *c* axis [Fig. 2(f)] is shown in the upper right panel of Fig. 1. Note that the number of the "charged" site in this model ($= 1/5$) is roughly consistent with the nominal number of the *d* electrons in this compound, $n = 0.18$. This charge/orbital ordering also induces a monoclinic distortion, which may be due to the fact that the charge/orbital ordering causes the localization of *d* electrons on the Ti ions and increases the effective ionic radius of the Ti ions [20]. It should also be pointed out that the periodicity of the Ba-ion ordering existing at high T in $\mathrm{Ba}_x\mathrm{Ti}_8\mathrm{O}_{16+\delta}$ is related to x, whereas that of the charge/orbital ordering is related to $n = (x - \delta)/4$. This means that the modulation in the Ti chain coexists but competes with the ordering of the Ba ions along the *c* axis, resulting in the complex behaviors of the superlattice peaks below T_c.

In conclusion, we found an exotic electronic phase transition at $T_c = 220$ K in $\mathrm{Ba}_x\mathrm{Ti}_8\mathrm{O}_{16+\delta}$, which is characterized by the modulation in the Ti chains and the spectral weight transfer of over 2 eV in the optical conductivity spectrum. These results indicate that the novel ground state of the present compound is dominated by the electron correlation effect and the coupling between the electronic structure and the lattice distortion.

This work was supported by JSPS KAKENHI Grant No. 25287090. The synchrotron radiation experiments were performed at BL02B2 in SPring-8 with the approval of the Japan Synchrotron Radiation Research Institute (JASRI) (Proposal No. 2014B1146).

---

[1] G. Grüner and A. Zettl, Phys. Rep. **119**, 117 (1985).
[2] N. Motoyama, T. Osafune, T. Kakeshita, H. Eisaki, and S. Uchida, Phys. Rev. B **55**, R3386(R) (1997).
[3] T. Osafune, N. Motoyama, H. Eisaki, and S. Uchida, Phys. Rev. Lett. **78**, 1980 (1997).
[4] P. Abbamonte, G. Blumberg, A. Rusydi, A. Gozar, P. G. Evans, T. Siegrist, L. Venema, H. Eisaki, E. D. Isaacs, and G. A. Sawatzky, Nature(London) **431**, 1078 (2004).
[5] K. Takenaka, K. Nakada, A. Osuka, S. Horii, H. Ikuta, I. Hirabayashi, S. Sugai, and U. Mizutani, Phys. Rev. Lett. **85**, 5428 (2000).
[6] N. E. N. E. Hussey, M. N. McBrien, L. Balicas, J. S. Brooks, S. Horii, and H. Ikuta, Phys. Rev. Lett. **89**, 086601 (2002).
[7] H. Yamada and Y. Ueda, J. Phys. Soc. Jpn. **68**, 2735 (1999).
[8] T. Yamauchi, Y. Ueda, and N. Môri, Phys. Rev. Lett. **89**, 057002 (2002).
[9] C. Presura, M. Popinciuc, P. H. M. van Loosdrecht, D. van der Marel, M. Mostovoy, T. Yamauchi, and Y. Ueda, Phys. Rev. Lett. **90**, 026402 (2003).
[10] M. Isobe, S. Koishi, N. Kouno, J. Yamaura, T. Yamauchi, H. Ueda, H. Gotou, T. Yagi, and Y. Ueda, J. Phys. Soc. Jpn. **75**, 073801 (2006).
[11] A. C. Komarek, M. Isobe, J. Hemberger, D. Meier, T. Lorenz, D. Trots, A. Cervellino, M. T. Fernández-Díaz, Y. Ueda, and M. Braden, Phys. Rev. Lett. **107**, 027201 (2011).
[12] K. Hasegawa, M. Isobe, T. Yamauchi, H. Ueda, J. I. Yamaura, H. Gotou, T. Yagi, H. Sato, and Y. Ueda, Phys. Rev. Lett. **103**, 146403 (2009).
[13] P. Mahadevan, A. Kumar, D. Choudhury, and D. D. Sarma, Phys. Rev. Lett. **104**, 256401 (2010).
[14] T. Toriyama, A. Nakao, Y. Yamaki, H. Nakao, Y. Murakami, K. Hasegawa, M. Isobe, Y. Ueda, A. V. Ushakov, D. I. Khomskii *et al.*, Phys. Rev. Lett. **107**, 266402 (2011).
[15] T. Ozawa, I. Suzuki, and H. Sato, J. Phys. Soc. Jpn. **75**, 014802 (2006).
[16] Z. Q. Mao, T. He, M. M. Rosario, K. D. Nelson, D. Okuno, B. Ueland, I. G. Deac, P. Schiffer, Y. Liu, and R. J. Cava, Phys. Rev. Lett. **90**, 186601 (2003).
[17] R. W. Cheary, Acta Crystallogr. Sect. B **46**, 599 (1990).
[18] T. Höche, P. Olhe, R. Keding, C. Rüssel, P. A. van Aken, R. Schneider, H.-J. Kleebe, X. Wang, A. J. Jacobson, and S. Stemmer, Philos. Mag. **83**, 165 (2003).
[19] K. Noami, Y. Muraoka, T. Wakita, M. Hirai, Y. Kato, T. Muro, Y. Tamemori, and T. Yokoya, J. Appl. Phys. **107**, 073910 (2010).
[20] In the hollandite structure ($\mathrm{A}_2\mathrm{B}_8\mathrm{O}_{16}$), a monoclinic distortion occurs when the ratio of the ionic radius of the B ion to that of the A ion (r_B/r_A) is larger than a certain value (~0.48) [41].
[21] The results for the No. 2 tetragonal sample and the monoclinic sample are shown in Supplemental Material at http://link.aps.org/supplemental/10.1103/PhysRevB.92.220408.

[22] T. Kanzaki, R. Kubota, and T. Katsufuji, Phys. Rev. B **85**, 144410 (2012).

[23] E. Nishibori, M. Takata, K. Kato, M. Sakata, Y. Kubota, S. Aoyagi, Y. Kuroiwa, M. Yamakata, and N. Ikeda, Nucl. Instrum. Methods Phys. Res. A **467-468**, 1045 (2001).

[24] K. Momma and F. Izumi, J. Appl. Crystallogr. **44**, 1272 (2011).

[25] Note that the contribution of T-independent Van Vleck paramagnetism is ignored in this estimation. According to F. E. Senftle and A. N. Thorpe, Phys. Rev. **175**, 1144 (1968), the van Vleck paramagnetic susceptibility of the Ti^{4+} ion is $\chi_{\mathrm{VV}} \sim 3 \times 10^{-5}$ $\mathrm{cm}^3/\mathrm{mol}$. Taking account of this χ_{VV}, the Curie-Weiss fitting gives $C = 0.14$ K $\mathrm{cm}^3/\mathrm{Ti}$ mol and $\theta = 197$ K above 220 K and $C = 0.082$ K $\mathrm{cm}^3/\mathrm{Ti}$ mol and $\theta = 63$ K below 150 K.

[26] D. Kuse and R. Zeller, Solid State Commun. **11**, 355 (1972).

[27] W. Kobayashi, Y. Hayashi, M. Matsushita, Y. Yamamoto, I. Terasaki, A. Nakao, H. Nakao, Y. Murakami, Y. Moritomo, H. Yamauchi *et al.*, Phys. Rev. B **84**, 085118 (2011).

[28] W. Koshibae, K. Tsutsui, and S. Maekawa, Phys. Rev. B **62**, 6869 (2000).

[29] These superlattice peaks were not observed in the synchrotron powder x-ray diffraction measurement shown in Fig. 2(a), probably due to their small intensities compared with those of the fundamental peaks.

[30] L. A. Bursill and G. Grzinic, Acta Crystallogr. Sect. B **36**, 2902 (1980).

[31] F. J. DiSalvo, J. V. Waszczak, and K. Yamaya, J. Phys. Chem. Solids **41**, 1311 (1980).

[32] Y. K. Kuo, C. S. Lue, F. H. Hsu, H. H. Li, and H. D. Yang, Phys. Rev. B **64**, 125124 (2001).

[33] R. S. Kwok and S. E. Brown, Phys. Rev. Lett. **63**, 895 (1989).

[34] X. Xu, A. F. Bangura, C. Q. Niu, M. Greenblatt, S. Yue, C. Panagopoulos, and N. E. Hussey, Phys. Rev. B **85**, 195101 (2012).

[35] D. W. Visser, A. P. Ramirez, and M. A.Subramanian, Phys. Rev. Lett. **78**, 3947 (1997).

[36] J. Q. Yan, J. S. Zhou, and J. B. Goodenough, Phys. Rev. Lett. **93**, 235901 (2004).

[37] T. Omura, T. Ishikawa, Y. Ishitsuka, and T. Katsufuji, Phys. Rev. B **86**, 054436 (2012).

[38] G. Li, W. Z. Hu, D. Qian, D. Hsieh, M. Z. Hasan, E. Morosan, R. J. Cava, and N. L. Wang, Phys. Rev. Lett. **99**, 027404 (2007).

[39] A. Sacchetti, L. Degiorgi, T. Giamarchi, N. Ru, and I. R. Fisher, Phys. Rev. B **74**, 125115 (2006).

[40] T. Ishikawa, K. Ookura, and Y. Tokura, Phys. Rev. B **59**, 8367 (1999).

[41] J. E. Post, R. B. V. Dreele, and P. R. Buseck, Acta Crystallogr. Sect. B **38**, 1056 (1982).